

Chromatic Contrast Discrimination: Data and Prediction for Stimuli Varying in L and M Cone Excitation

Vivianne C. Smith,* Joel Pokorny, Hao Sun

Visual Sciences Center, The University of Chicago, Chicago, Illinois 60637

Received 9 November 1998; accepted 5 August 1999

Abstract: Chromatic discrimination data are presented for pulsed and steady stimuli as a function of surround chromaticity and structure. All stimuli and surrounds were at equiluminance and at a constant level of short-wavelength-sensitive cone excitation. The test stimulus was a square array of four 1° squares. A 0.07° crosshair of the same chromaticity as the surround separated the squares. Both the test stimuli and the surrounds varied in relative excitation of the long-wavelength and middle-wavelength sensitive cones. When stimuli briefly replaced a portion of a steadily viewed background (the Pulse Paradigm), the discriminations were optimal at the background chromaticity and degraded for chromaticities away from the background. The discrimination steps were independent of the background size, which varied from a spatially extensive display to one matching exactly the appearance of the test array. Discrimination was determined only by the spatio-temporal chromatic contrast of the stimulus relative to the background. When the stimuli were presented continuously within a surround (the Pedestal Paradigm), discrimination was still determined by the surround chromaticity, independent of the surround size. Even a narrow 0.07° crosshair was sufficient to establish optimal discrimination at the crosshair chromaticity. With the surround and crosshair dark, spectral opponent channels maintained an intrinsic normalization near equal energy white. There was little indication of adaptation to the test stimuli. The data were fit by a model of spectral opponency linking detection and discrimination as a function of both retinal illuminance

level and chromaticity. The model is explicitly based on observations of the behavior of retinal ganglion cells of the Macaque retina. The model incorporates well-accepted psychophysical concepts that adaptation in cone spectral-opponent channels occurs at multiple sites both before and after spectral opponency. © 2000 John Wiley & Sons, Inc. *Col Res Appl*, 25, 105–115, 2000

Key words: adaptation; color; discrimination; opponency; model

INTRODUCTION

Chromatic discriminative ability is an important feature of color specification, and this is reflected in the numbers of studies of such ability in the scientific literature. In early studies of wavelength and colorimetric purity discrimination (reviewed in Pokorny and Smith,¹ the stimuli were usually presented as abutting standard and test fields. For wavelength discrimination, the observer adjusted the test wavelength to achieve a just-noticeable difference from the standard wavelength. For least colorimetric purity, the observer adjusted the proportion of a standard wavelength in a mixture with the instrument white to achieve a just-noticeable difference from the instrument white. Although such data are usually presented as the $\Delta\lambda$ or as the least reciprocal colorimetric purity plotted as a function of the standard wavelength, Wright² showed that the data could be unified by plotting them as distances in a chromaticity diagram. Additionally, Wright measured just-noticeable differences along arbitrary lines in color space. This approach culminated in the MacAdam ellipses³ that were collected as color matches to a fixed set of standards of constant luminance. The ellipses were obtained as the standard deviation of repeated color matches to each of 25 chromaticities widely spaced in the C.I.E.⁴ chromaticity diagram.

* Correspondence to: Dr. Vivianne Smith, Visual Sciences Center, University of Chicago, 939 East Fifty-Seventh St., Chicago, IL 60637 (e-mail: vc-smith@uchicago.edu)

Contract grant sponsor: USPH NEI

Contract grant number: EY07390

© 2000 John Wiley & Sons, Inc.

Two theoretical ideas dominated the thinking about analysis and prediction of the data. Many trichromatists favored the line element theory, postulated by Helmholtz,⁵ and developed by Schrödinger⁶ and later Stiles⁷ among others (reviewed by Stiles⁸). In line element theory, the signals generated by three independent cone types, the short- (*S*), medium- (*M*) and long- (*L*) wavelength cones were subject to weights reflecting the radiance and quantal catch rate, the adaptational state, threshold noise, number, or other considerations such as spatio-temporal parameters. Most versions of line element theory assume that the cones are in the Weber region at the photopic levels of discrimination measurement. A threshold occurred when the summed differences for each cone-type from the standard level reached a fixed criterion level. The attraction of this approach lay in the fact that it treated chromaticity discrimination in the same manner as increment thresholds in the luminance domain, thus providing a unified theory of detection and discrimination for the entire luminance range of photopic vision. Jameson and Hurvich developed an alternate approach rooted in opponent process ideas.⁹ They presented a chromatic opponent plane as a linear transform of color-matching data with normalization to the equal energy white. This provided an intuitive and simple description of chromaticity discrimination. However, the plane needed to be reparameterized for each luminance level and for changes in normalization chromaticity.

LeGrand¹⁰ evaluated the MacAdam ellipses in terms of trichromatic theory. In making this calculation, he assumed that luminance was determined only by the sum of *L* and *M* cone responses. This simplification allowed him to calculate only the *S* and *L* cone excitation axes passing through each ellipse center; the *M* cone excitation level was directly calculable from *L*. He then plotted the size of the arc through the ellipse as a function of the excitation at the center. The data for *S* cones had the shape of an increment threshold function, a result consistent with line element theory. The data for *L* and *M* cones showed a trade-off of *L* and *M* cone excitation. The data could be summarized by plotting the discrimination step as a function of the *L/M* ratio; discrimination was optimal when the cone excitations were balanced. Subsequently, Stiles⁸ noted that the existence of a minimum was inconsistent with line element theory, even if a subtractive opponent process was added following a stage of cone-specific Weber adaptation.

Boynton and Kambe¹¹ studied chromaticity discrimination using modern cone axes^{12,13} and equiluminant stimuli. Their data confirmed the LeGrand analysis: for discriminations mediated by *L* and *M* cones, there is an intrinsic normalization near equal energy white, even when chromatic stimuli are presented continuously in the dark. In contrast, for discriminations mediated by *S* cones, the data have the appearance of an increment threshold function.¹¹ Boynton and Kambe introduced a new normalization of the MacLeod and Boynton space¹³ with a scheme they called cone trolands. The *L* and *M* normalization was retained; the *S* cone normalization was changed so that for an illumination metameric to equal energy white, *S* was set equivalent

to *Y* and called *S* tds. This normalization allows presentation of data either in (*l*, *s*) chromaticity units or in (*L*, *S*) cone-troland units. In the latter form, the units remain traceable to the physical calibration. Cone troland units are particularly useful in evaluating physiologically based models of chromatic detection and discrimination.¹⁴

In the past two decades, there have been major advances in the understanding of retinal anatomy and electrophysiology (reviewed by Lee¹⁵ and Dacey *et al.*¹⁶). The circuitry has three pathways, each consisting of groups of cells that feed signals forward from the photoreceptor to the lateral geniculate nucleus, via bipolar and ganglion cells, with output to the visual cortex. The parvo-cellular pathway mediates spectral opponency of *M* and *L* cones. Four subgroups of parvocellular cells have been defined, by characteristic response patterns,^{17,18} reflecting the center activity of the typical center-surround retinal ganglion cell. The anatomical micro-circuitry of these four subtypes has not yet been discovered. As with classically defined center-surround cells,¹⁹ On-center cells respond to an increase and Off-center cells to a decrease in luminance contrast on their centers.²⁰ The cell types are further divided by their chromatic properties.^{17, 18} The *L*-On-center and the *M*-Off-center cell responds to an increase in *L* td contrast (“reddish” appearing lights) and the *M*-On-center and the *L*-Off-center cell responds to an increase in *M* td contrast (“greenish” appearing lights). Another class of spectral opponency is shown by the konio-cellular pathway $+S - (L+M)$ cells, which combine inputs from *S*, *M*, and *L* cones.²¹ The third major pathway from retina to cortex is the nonopponent magno-cellular pathway, which sums inputs of *M* and *L* cones in either On- or Off-center receptive fields.

In this article, we present a model to describe how the parvo-cellular pathway might participate in chromaticity discrimination mediated by *M* and *L* cones. We have measured chromaticity discrimination for equiluminant stimuli in chromatic surrounds. We first measured chromaticity discrimination for pulsed stimuli in order to parameterize the model. Then we measured chromaticity discrimination for steadily presented stimuli in order to evaluate conditions, which more nearly approximate those encountered in everyday experience. The experimental displays were generated on color monitor systems. Stimulus chromaticity specification was in a relative cone troland space, and the data are presented in cone trolands.¹⁴ Abstracts of the data have been published elsewhere.²²⁻²⁴

METHODS

Apparatus and Calibration

The stimuli for the initial experiments were generated by a PIXAR II image processor under control of a SUN 3 computer and were displayed on a 17" Nanao (T560i Flexscan) color monitor. Stimuli in later experiments were generated by a Radius Thunder 30/1600 card under control of a Macintosh PowerPC 9500/132 and displayed on a 17" Radius PressView 17 SR monitor. Calibration procedures and

stimulus specification were identical for both systems. The phosphor output was measured as a function of wavelength at the maximum light level for each phosphor using an International Light model IL1700 Spectroradiometer/Photometer. Radiance was measured (4.2 nm half-bandwidth) at wavelength intervals of 0.83 nm and then converted to 1 nm intervals by interpolation. The stimuli were specified in a cone chromaticity space (l, s, Y_J), using the Smith and Pokorny transformation¹² of the Vos–Judd²⁵ observer, (x_J, y_J, Y_J). Normalization was to the relative troland space.¹¹ In this normalization, $\bar{l}(\lambda) + \bar{m}(\lambda) = \bar{y}_J(\lambda)$, and the $\bar{s}(\lambda)$ fundamental is equivalent to $\bar{z}(\lambda)$. Thus, 100 tds of equal energy white are partitioned among 66.54 L trolands and 33.46 M trolands and the S troland content is 100. The chromaticity coordinates and maximal luminance (cd/m^2) of the phosphors in this relative cone troland space (l, s, Y_J) at equal energy white were: Red: (0.815, 0.12, 2.19); Green: (0.607, 0.218, 8.80); and Blue: (0.526; 10.321; 1.01) for the PIXAR/SUN system, and Red: (0.825, 0.091, 3.23); Green: (0.613, 0.151, 7.81); and Blue: (0.525, 10.30, 0.96) for the MAC/Radius system.

The luminance of each phosphor was measured for 1024 levels of input integer value with the spectroradiometer/photometer. Look-up tables were constructed to represent relations between voltage integer values and phosphor luminances. Transformation between cone relative troland values (l, s, Y_J) and voltage integer values of the three phosphors was performed using the results of the measurements and calculations.

The surround and test chromaticities were arranged on a constant s -line in (l, s) relative cone troland space with a relative s -troland value of 1.0, metameric to equal energy white at an l -chromaticity of 0.665. There were a series of test stimuli on the l -line, spaced between 0.62 and 0.79. There were three surrounds on the l -line; a control surround had an l -chromaticity of 0.665. Two biased surrounds had l -chromaticities near 0.61–0.62 and 0.74–0.81. The exact l -chromaticities of the tests and surrounds varied slightly in different experiments.

The test stimulus was a square array of four 1° squares with a small separation of 4 pixel elements. In the initial experiments the separations were 0.05° . In subsequent experiments, different spatial resolution of the monitor system gave a visual angle of 0.07° . The luminance of the stimuli and their surrounds was kept at 12 cd/m^2 throughout the experiment. This luminance corresponded to 115 effective trolands.²⁶ The monitor screen was viewed directly at 1 m. A spatially extensive ($9.2^\circ \times 8.7^\circ$) surround was used in Experiment 1. In Experiment 2, the surround size was varied from spatially extensive ($14.8^\circ \times 11.2^\circ$) to $2.07^\circ \times 2.07^\circ$ and in Experiment 3 it was $2.07^\circ \times 2.07^\circ$ (the size of the four-square array).

Procedure

Two paradigms were used (Fig. 1). The paradigms differed only in the display preceding the trial; the trials presented identical stimuli.

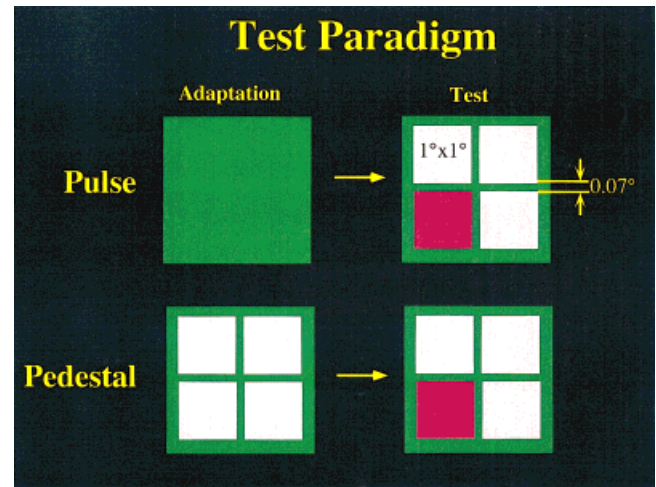


FIG 1. Display sequence for the (upper) Pulse and (lower) Pedestal Paradigms. The left figures show display appearance during adaptation and inter-trial intervals; the right figures show appearance during a trial.

(1) Pulse Paradigm: The surround chromaticity was presented continuously as a background (Fig. 1, upper left); the four-square array was present only during the trial, replacing its portion of the background (Fig. 1, upper right). Three squares were presented at a fixed, test chromaticity; the fourth had an increment or decrement added to the test chromaticity. The chromaticity change of all four squares followed a raised cosine of 1.5 s duration. Between trials, the observer maintained adaptation to the uniformly illuminated background chromaticity.

(2) Pedestal Paradigm: the four-square array was present continuously at a fixed test chromaticity (Fig. 1, lower left). During the trial, one square changed as an increment or decrement in chromaticity following a raised cosine of 1.5 s duration (Fig. 1, lower right). Between trials, the observer maintained adaptation to the surround and test chromaticities. In the case of the smallest surround (equivalent to the four square array), the only indication of the surround presence was in the cross-shaped separation between the four squares.

The observer first adapted for 3 min to the chosen surround and paradigm display. A fixation dot provided a fixation guide and served to signal the trial occurrence. At the start of a trial, the dot disappeared. Each trial presented three test squares with the fourth square at a different chromaticity. At the trial conclusion, the fixation dot reappeared together with the cursor.

In Experiment 1, we used a discrimination judgment; the observer used the mouse to place the cursor in the stimulus position judged “different.” A mouse click at this position stored the result and reset the display for the next trial. A correct response stored the result and reset the display for the next trial. In experiments 2 and 3, we used an identification judgment. The observer used the mouse to place the cursor in the stimulus position judged to be “different” and additionally indicated the direction of the difference as either in a positive 1 (“redder” or less “green”) direction or

a negative l-chromaticity direction (“greener” or less “red”). A correct (position and direction) response stored the result and reset the display for the next trial. There was no difference in the thresholds for detection and for identification.²⁷

Trials followed a double random alternating staircase. In one staircase the threshold chromaticity was measured in an increment direction; in the other, in a decrement direction from the chosen test chromaticity. Pilot data established that there were no systematic differences between increment and decrement thresholds. On the initial trials of the staircase, an easily discriminable step was present. The step size decreased systematically until a criterion step size was reached. The criterion was set in pilot studies to produce an efficient staircase, requiring about 40–50 trials to produce ten reversals. Ten reversals were measured for both the increment and the decrement staircases. The averages of the ten reversals were stored as increment and decrement thresholds. A 45-min session allowed measurement of increment and decrement thresholds at five test chromaticities. Thus, two sessions were required to obtain full data for one surround chromaticity and one paradigm. The entire paradigm was repeated, and reported data are the average of two increment and two decrement thresholds for each test chromaticity and for each surround. The data were stored as the relative *l*-troland chromaticity at threshold and re-expressed as the ΔL troland at threshold, $115(l_{thr} - l_{test})$ plotted vs. the test chromaticity in *L* trolands.

Observers

There were a total of five observers (AC, male, 30; GK, female, 21; HS, female 35; VS, female 56; YH, male 33), who were all normal trichromats as assessed with the Ishihara pseudo-isochromatic plates and the Neitz OT anomaloscope. There was no history of X-chromosome linked color defect in the families of the female observers. Farnsworth–Munsell 100-hue error scores were 20 for AC, 24 for GK, 4 for HS, 4 for VS, and 8 for YH. AC, GK, and YH were well-practiced psychophysical observers, but had no knowledge of the experimental design or expectation. HS and VS are among the authors. At least two observers ran the complete paradigms for each experiment. Confirmatory data were obtained on a third observer.

MODEL

We developed a model of chromatic discrimination for the Pulse Paradigm based on physiological data of the spectral opponent Parvo-cellular (PC-) pathway of primates.^{17, 18, 28} The model, sketched in the top row of Fig. 2, postulates an early stage of cone-specific multiplicative adaptation followed by spectral opponency, which incorporates a stage of subtractive feedback at the site of spectral opponency. A conceptually similar version of this approach was proposed for SWS cone discrimination mediated by konio-cellular pathway by Zaidi, Shapiro, and Hood.²⁹ For the Pulse Paradigm, the cells stimulated by the display are adapted to

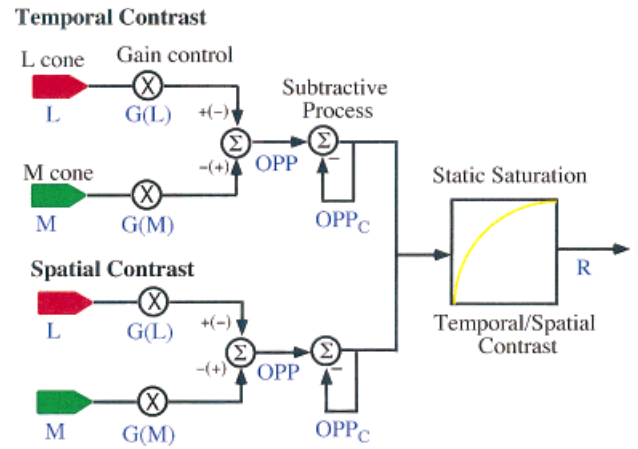


FIG 2. A diagram of the PC-pathway model. Upper portion shows model for the Pulse Paradigm. Lower portion adds a second state of adaptation and resulting spatio-temporal contrast for the Pedestal Paradigm.

the display. The trial creates a spatio-temporal contrast event in the test array from the fixed adaptation level.

Studies of increment detection on steady backgrounds^{30, 31} have revealed cone-specific adaptation for *L*- and *M*-cones. In our application, the multiplicative stage does not produce Weber’s Law, leaving a net signal at the spectral opponent stage. Chromatic temporal sensitivity data measured as a function of retinal illuminance level in both psychophysics³² and physiology²⁸ indicates a need for a partial rather than a complete multiplicative gain term. Subtractive feedback then cancels the majority of the net signal to the adaptation chromaticity. The need for subtractive feedback is demanded by psychophysical chromatic discrimination data and by physiology.³³ Following the spectral opponent stage, the response to a chromatic contrast change from the adapting chromaticity follows a static saturation function. A static saturation function describes retinal ganglion cell responses to contrast changes from their adapted steady-state level.^{18, 34} This general model is based on ideas published in both the luminance literature^{35–38} and the chromaticity discrimination literature.^{39,40}

The response of a spectral opponent cell to a chromaticity change, C from a fixed adapting chromaticity, A is:

$$R = R_{max}[OPP_C/(OPP_C + SAT)], \quad (1)$$

where OPP_C is a spectral opponent term and SAT is the static saturation. We assume the spectral opponent term is subject to subtractive feedback determined by the opponent signal at the adapting chromaticity.

$$OPP_C = OPP_T - k_1 OPP_A, \quad (2)$$

where OPP_T is the spectral opponent term at the test chromaticity, OPP_A represents the spectral opponent term at the adapting chromaticity, and k_1 represents the subtractive feedback strength. Psychophysical studies⁴¹ of luminance thresholds have suggested that subtractive feedback can be as high as 90%.

The cone spectral opponent term can be derived for each

of the four subtypes of PC-pathway cell, (+LWS–MWS), (+MWS–LWS), (–LWS+MWS), and (–MWS+LWS). For a (+LWS–MWS) cell, the spectral opponent term at the test chromaticity would be given by

$$OPP_{(+LWS-MWS)} = [L_T/l_{max}G(L_A/l_{max}) - k_2M_T/m_{max}G(M_A/m_{max})], \quad (3)$$

where L_T and M_T represent cone trolands at the test chromaticity,¹⁴ L_A and M_A represent the cone trolands at the adapting chromaticity, l_{max} and m_{max} are the maximal sensitivities of the Smith and Pokorny¹² cone fundamentals. The L and M cone trolands sum to the total retinal illuminance level, which is usually constant in any measurement of chromatic discrimination. The constant k_2 represents the surround strength of the spectral opponency. In retinal ganglion cell data, the surround strength for PC-pathway cells varies from 0.7–1.0.⁴² The strength of the opponent signal is governed by the multiplicative gain at the first site. $G(L_A/l_{max})$ and $G(M_A/m_{max})$ are multiplicative gain terms at the adapting chromaticity, given by an equation of the form:

$$G(L) = 1/(1 + k_3L_A/l_{max})^{k_4}, \quad (4)$$

where L_A is in cone trolands and k_3 , k_4 are constants. Independent estimation of k_3 and k_4 requires evaluation of chromaticity discrimination as a function of radiance.

If the subtractive term does not remove the entire effect of the adapting chromaticity, there will be some residual signal at the adapting chromaticity. Provided that the criterion for a threshold, δ , is small relative to R_{max} , the chromatic discrimination threshold for an optimal spatio-temporal stimulus at the adapting chromaticity can be written based on the derivative to Eq. (1):

$$\log(\Delta L_A) = \log(\delta/R_{max}) - \log[1/(G(L)/l_{max}) + 1/(G(M)/m_{max})] + \log[(OPP_A + SAT)^2/SAT] \quad (5)$$

where the second term represents the luminance gain response, and the third term represents the opponent term. The threshold at other test chromaticities depends on the size of the contrast step ΔOPP , between the adapting and the new test chromaticity. This introduces an additional term, ΔOPP , modifying Eq. (5):

$$\log(\Delta L_C) = \log(\delta/R_{max}) - \log[1/(G(L)/l_{max}) + 1/(G(M)/m_{max})] + \log[\Delta OPP + OPP_A + SAT]^2/SAT]. \quad (6)$$

An optimal test stimulus for chromaticity detection is of low spatio-temporal frequency, e.g., a 2°, 1 s pulse with blurred spatio-temporal edges. In pilot studies, we noted that use of brief durations or small test spots raises thresholds by a constant, independent of the adaptation variables. Use of a complex spatial pattern, a pseudo-isochromatic plate design with continuous view similarly raised thresholds by a constant.⁴³

A given PC-pathway cell responds best to a chromaticity change in its preferred direction.^{18,44} Change in the nonpre-

ferred direction drives the cell below its resting level. The resting level is usually only about 15% of the maximal response rate. This is an intrinsic nonlinearity that renders the cell response asymmetric: the cell behaves as if partially rectified. The (+L–M) cell responds to increases in “redness” and increases in luminance contrast, the (–L+M) cell responds to decreases in “redness” and decreases in luminance contrast, the (+M–L) cell responds to increases in “greenness” and increases in luminance contrast, the (–M+L) cell responds to decreases in “greenness” and decreases in luminance contrast. All four cell types respond to equiluminant chromatic temporal alternation, differing only in the phase of their responses.^{17,28,42} For equiluminant chromatic pulses, the (+L–M) and (–M+L) give redundant information, responding positively to “redward” changes from their adaptation point; similarly the (+M–L) and (–L+M) give redundant information, responding positively to “greenward” changes from their adaptation point.¹⁸ To achieve a response for the entire chromatic contrast range, we require pairs of cells of opposite chromatic signatures, e.g., (+L–M) and (+M–L). Thus, in using Eq. (6), we used a (+L–M) to predict chromaticity discrimination for pulses with “redward” direction ($L > L_A$) from the adaptation chromaticity and a (+M–L) for pulses with “greenward” direction ($L < L_A$) from the adaptation chromaticity.

RESULTS

Observers AC and VS ran the Pulse and Pedestal Paradigms on both sets of equipment using similar surround and test chromaticities. We noted no differences in thresholds attributable to the display system.

Experiment 1: Data with a Spatially Extensive Surround

Our initial goal was to develop the model and then compare the Pulse and Pedestal Paradigms. The model detailed above was designed to predict data for the Pulse Paradigm for which the observer was adapted to the surround chromaticity, and the chromaticity contrast steps were presented as a brief cosine excursion. Data were collected on three observers (AC, GK, VS) using the Pixar/SUN system (surround: 9.2° × 8.7°) and four observers (AC, HS, YH, VS) with the Radius/Mac system (surround: 14.8° × 11.2°). The l -chromaticities of the surround were 0.6077, 0.6654, and 0.813 for the Pixar/SUN system and 0.62, 0.6654, and 0.74 for the Radius/Mac system.

Results Figure 3 shows results for observer AC and the Pulse Paradigm. Each panel shows a different surround chromaticity. The average data (\pm 2 s.e.) for the Pulse Paradigm are shown as closed symbols, plotted as a function of the test chromaticity. For each surround, the minimum threshold occurred at or near the surround chromaticity. The thresholds increased as the test chromaticity moved away from the surround. With a surround metameric to the equal energy spectrum, the data gave a characteristic V-shape as

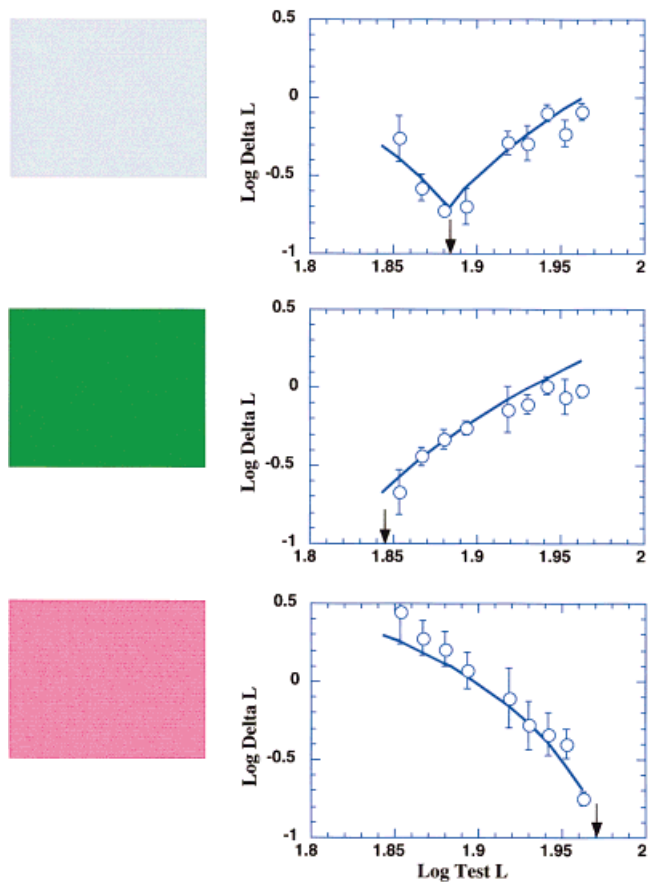


FIG 3. Discrimination data for a large, rectangular surround and the Pulse Paradigm (observer AC). The surround L -chromaticities are shown by arrows on the abscissa of each plot: (upper panel) 0.61, (middle panel) 0.665, and (lower panel) 0.81. The dashed line is the model fit [Eq. (6) in the text]. Icons on left show display appearance (not to scale) during adaptation and inter-trial interval.

described in the literature.^{40, 45} At the surround chromaticity, the threshold was about $0.2 L$ tds, similar to data of Yeh, Pokorny, and Smith⁴⁶ and Miyahara, Smith, and Pokorny,⁴⁰ who also used a forced choice method; but more sensitive than the study of Boynton and Kambe¹¹ ($1 L$ td), who chose a method designed to give large threshold steps. There was little variation among the five observers except for the overall vertical scaling, indicative of inter-observer variation in criterion.

The data for the Pulse Paradigm were fit by Eq. (6). To reduce the number of free parameters, we set values for k_1 – k_4 based on literature data. Properties of the spectral opponent channel were based on physiological work; we set k_1 at 0.90 and k_2 at 0.80. Since the data were collected only at a single retinal illuminance level, there is no independent factor to constrain the value of k_3 – k_4 . Using psychophysical data of Miyahara *et al.*,⁴⁷ we fixed k_3 at 0.33 and k_4 at 0.75. Thus, the fits were constrained to 2 free parameters, (δ/R_{max}) and SAT . We fit data from the three chromatic surrounds simultaneously; forty thresholds determined the fit. The fits are shown as dashed lines. The inter-observer values of

(δ/R_{max}) varied from 0.017–0.025 and the values of SAT varied from 2.8–4.3.

The average data (± 2 s.e.) for AC using the Pedestal Paradigm are shown in Fig. 4. Thresholds at the surround chromaticity are a replication of the Pulse Paradigm thresholds. Data obtained for the Pedestal Paradigm with the test stimuli in continuous view showed, at least for observer AC, mild flattening of the V-shape compared with the data of the Pulse Paradigm (Fig. 3). The thresholds at a given chromaticity contrast step were slightly more sensitive than for the Pulse Paradigm. The flattening was intermediate for HS and minimal for observers GK, VS, and HY. It is further noted that the test stimuli did not disappear during the steady adaptation period. In an equiluminant display, the stimulus array tends to fade in the surround, especially when the chromatic contrast is small or the border is blurred. Our observers were instructed to maintain fixation between trials, but they were allowed to blink to maintain field appearance.

How might Eq. (6) be modified to account for the data? The solid lines on Fig. 4 show two potential models, based on the idea that discrimination is mediated by the state of cells stimulated by the test array. One hypothesis is that there is cone-specific adaptation to the test stimuli and that

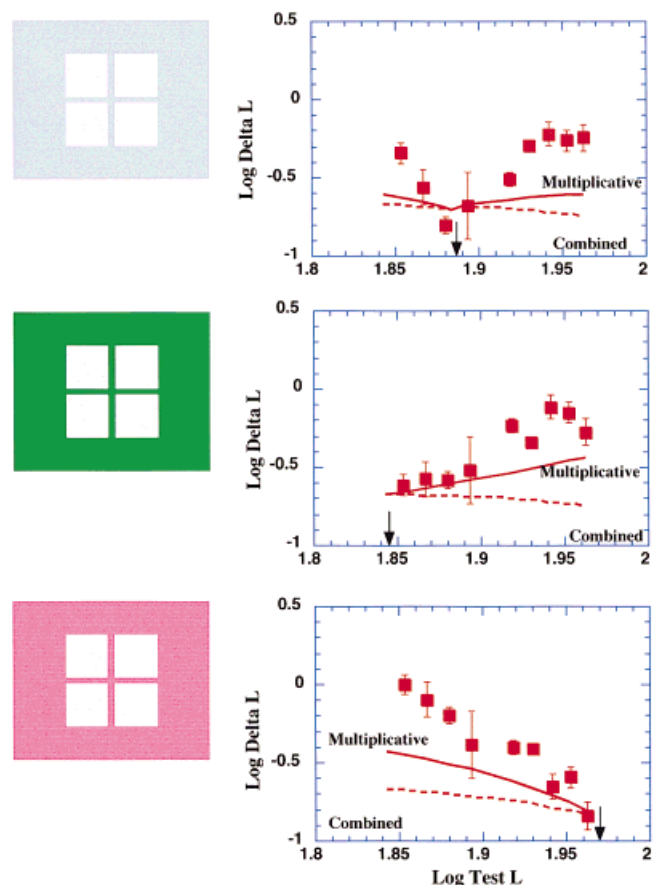


FIG 4. Discrimination data for a large, rectangular surround and the Pedestal Paradigm (observer AC). Panels are as in Fig. 3. The solid and dashed lines are possible models. Icons on left show display appearance (not to scale) during adaptation and inter-trial interval.

the subtractive adaptation of the spectral opponent signal is also local and determined by the chromaticity of the test stimuli. This would mean that OPP_A would be replaced by OPP_T in Eq. (2) and L_A would replace L_T in Eq. (4). This calculation with all other parameters fixed at the optima for the Pulse Paradigm generates a prediction with a slight negative slope. The prediction does not describe our data, but is observed for data collected when surround chromaticity is varied and a Pulse Paradigm is used, e.g., Krauskopf.⁴⁵

A second hypothesis is that there is cone-specific adaptation to the test stimuli, but the subtractive adaptation remains controlled by the surround. This could occur, if the multiplicative adaptation occurred within the cone photoreceptor itself, but the subtractive adaptation was governed by widespread interactions at a postreceptoral stage. This would mean that the L_A would be replaced by L_T in Eq. (4). This calculation with all other parameters fixed at the optima for the Pulse Paradigm is shown by dashed lines and shows a shallow V-shape. The prediction does not describe the data of observer AC.

The lower part of Fig. 2 shows the more complex situation of the Pedestal Paradigm. Now, cells under the test array are stimulated by the test chromaticity, while cells under the surround are stimulated by the surround chromaticity. Continuous spatial contrast is generated at the border. Suppose that this spatial contrast signal determines discrimination. The Pedestal Paradigm data can be fit using Eq. 6, but allowing some reduction in the spatial contrast signal. To fit the data, it is convenient to decrease the strength of the opponent contrast signals used in Eq. (6) by rewriting Eq. (2):

$$OPP_C = OPP_T - k_1(p OPP_A + (1 - p)OPP_T), \quad (7)$$

where p is the proportion of surround chromaticity in the subtraction. The solid lines show these fits. The values of p were 0.59 for observer AC, 0.96 for GK, 0.65 for HS, and 1.0 for HY and VS.

Discussion

The data for the Pulse Paradigm are fit well by the model equations. We maintain a constant state of adaptation and the chromatic contrast threshold is determined by the size of the spatio-temporal chromatic contrast step. We noted a trade-off between the amount of cone-specific adaptation and the amount of opponent subtraction. If cone-specific adaptation followed Weber's law, there would be no requirement for opponent subtraction. Adaptation to the surround chromaticity would be accomplished by the multiplicative term. Our choice of an exponent of 0.75 was based on literature data.^{28,32,47} An exponent less than 1.0 provides an intermediate level of chromatic adaptation. Subtractive feedback is then required to generate the symmetrical arms of the V-shape with a minimum near the adapting chromaticity that is characteristic of the data.

For the Pedestal Paradigm, we eliminate the large temporal contrast step of the entire stimulus array. The spatial chromatic contrast is present continuously. The data, how-

ever, are relatively little affected. Two interpretations of the data are evident. First, the large surround maintains the adaptation state for the task. At a retinal level this behavior does not occur.³³ In PC-pathway retinal ganglion cells, adaptation is virtually complete, both in luminance and chromaticity to a stimulus covering both center and surround. PC-pathway receptive fields near the fovea are so small that it is impossible to put a stimulus solely on the center. Nonetheless, it is conceivable that cortical receptive fields with larger summation areas could control chromatic discrimination under conditions of the Pedestal Paradigm.

Second, it is possible that discrimination is determined at the border between test and surround. Chromatic temporal alternation generates large signals in PC-pathway cells,²⁸ and this temporal alteration may mimic sweeping a target back and forth across a small receptive field in a spatial display. For a "white" surround and a "red" test field, it would be the +L-On-center cells that would respond vigorously as the chromatic contrast increased. In this view, cells adapted to the surround maintain the adaptation state and generate chromatic contrast across the spatial border. This interpretation is consistent with the observation that we saw little fading in our paradigm. In order to distinguish these interpretations, we next investigated the effect of decreasing surround size.

Experiment 2: Variation of Surround Size

Data with varying surrounds were collected with the MacIntosh–Radius system and observers HS and HY. The l -chromaticities of the surround were 0.62, 0.6654, and 0.74; there were 8 test chromaticities with l -chromaticities between 0.62–0.76. There were three surround sizes including $4.0^\circ \times 4.0^\circ$, $2.21^\circ \times 2.21^\circ$, and $2.07^\circ \times 2.07^\circ$ square. The $2.21^\circ \times 2.21^\circ$ surround appeared as an 0.07° border around the four-square array in the Pedestal Paradigm; for the $2.07^\circ \times 2.07^\circ$ surround, only the central, cross-shaped separation between the squares was visible during the Pedestal Paradigm.

If the V-shape observed in the Pedestal Paradigm was maintained by large adaptation pools, we would expect to see the V-shape flatten as surround size decreased. If the V-shape was maintained by chromatic contrast signals generated across the border, the V-shape should not be affected by surround size as long as a contrast border was present.

Results

Figure 5 shows data for observer HS comparing the Pulse and Pedestal Paradigms for a spatially extensive $14.8^\circ \times 11.2^\circ$ surround. Figures 6–8 show a similar comparison for the three smaller surrounds. The data for the Pulse Paradigm do not vary as a function of surround size. Equation (6) was fit to each dataset. The values of (δ/R_{max}) varied from 0.024–0.026 and the values of SAT varied from 2.49–2.63 for HS. Data for YH were more scattered, and the fits were not as good as for any of the other observers. The values of (δ/R_{max}) varied from 0.027–0.035 and the values of SAT varied from 2.51–4.34 for HS.

The data for the Pedestal Paradigm were similarly inde-

Surround: 14.8°x11.2°

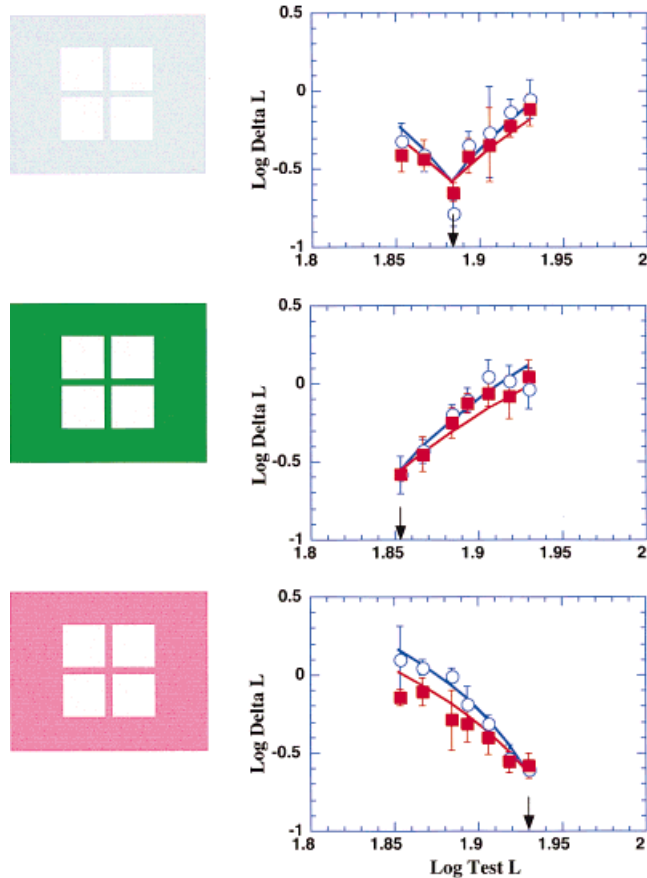


FIG 5. Discrimination data for a large, rectangular surround comparing the Pulse and Pedestal Paradigms (observer HS). The surround l -chromaticities are shown by arrows on the abscissa of each plot: (upper panel) 0.62, (middle panel) 0.665, and (lower panel) 0.74. Open circles in blue show data for Paradigm 1; closed squares in red show data for Paradigm 2. Icons on left show display appearance (not to scale) during adaptation and inter-trial interval for the Pedestal Paradigm.

pendent of surround size. Of the 24 conditions (8 test chromaticities and 3 surround chromaticities), only two sets of thresholds showed a lack of overlap as a function of surround size. These data were fit with Eq. (7) used to determine OPP_C in Eq. (6). The values of p in Eq. (7) varied from 0.55–0.75 for HS and 0.45–1.0 for YH. There was a small but consistent tendency for p to be higher for the two larger surround squares (4.0° and 8.0°) than for the two smaller surround squares (2.07° and 2.21°). This phenomenon may reflect an interaction with the display size, which required more careful fixation for the smaller displays.

Discussion The Pulse Paradigm data were not affected by the variation in surround size. This result was expected, because we maintained constant adaptation and the stimulus always presented a large spatio-temporal chromaticity contrast step. The Pedestal Paradigm data indicate that surround size was not an important factor in determining chromatic contrast discrimination. Even the presence of a 0.07° crosshair, between the discrimination squares was sufficient for

the crosshair chromaticity to control the discrimination function. The result is consistent with the notion that signals generated at test field borders determine discriminability.

Experiment 3: Adaptation to the Stimulus Array

As a control condition for Experiment 2 and to compare our data with other literature data, we allowed adaptation only to the stimulus array. The narrow separations between the four squares and the surround appeared dark. These data were collected with the Macintosh–Radius system and observers HS and HY. The chromaticities of the background and test stimuli were identical to those of Experiment 2. In this experiment, data for the Pulse Paradigm were collected with adaptation to one of the three surround chromaticities of Experiment 2. Data for Pedestal Paradigm were collected with adaptation to the test chromaticity.

Results Figure 9 shows data for observer HS following the format of Fig. 6. The data for the Pulse Paradigm gave similar results to data of Experiment 2 and were fit with Eq. 6. The value of (δ/R_{max}) was 0.022 (HS) and 0.023 (HY), and the value of SAT was 3.3 (HS) and 6.5 (HY). These

Surround: 4°x4°

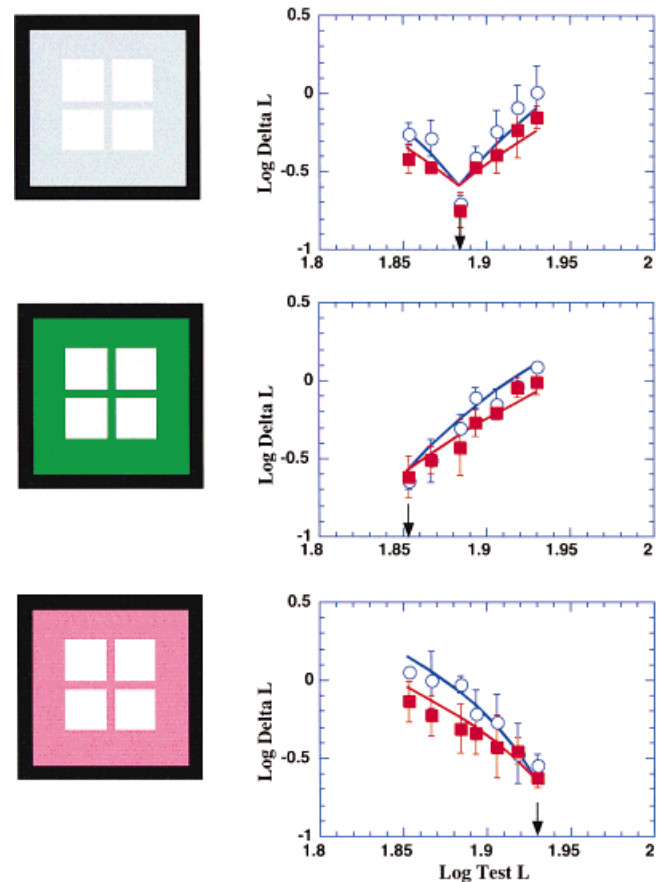


FIG 6. Discrimination data for a $4^\circ \times 4^\circ$ surround comparing both paradigms (observer HS). Format follows Fig. 5. Icons on left show display appearance (to scale) during adaptation and inter-trial interval the Pedestal Paradigm.

Surround: $2.21^\circ \times 2.21^\circ$

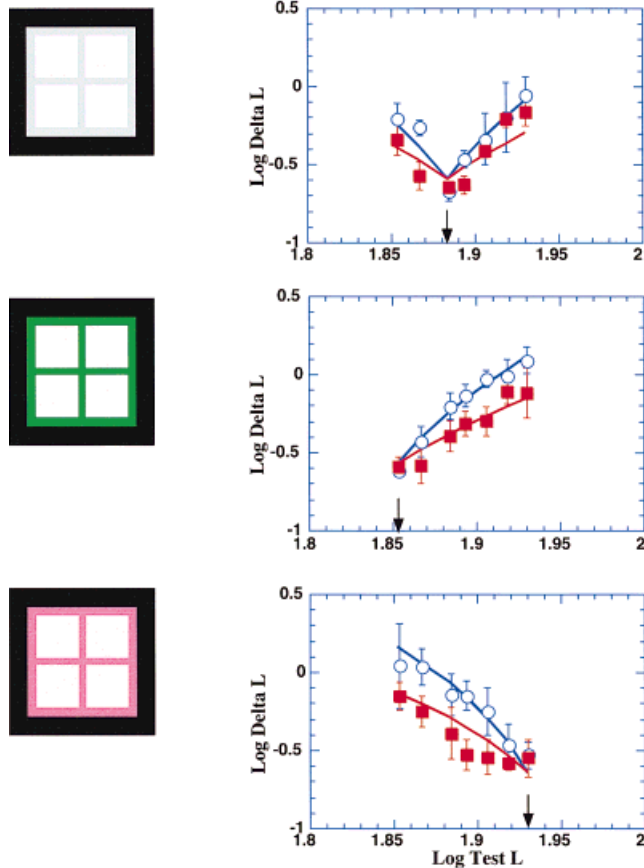


FIG 7. Discrimination data for a $2.21^\circ \times 2.21^\circ$ surround comparing both paradigms (observer HS). Format follows Fig. 6.

SAT values are slightly higher than those obtained in Experiment 2, indicating a slight shallowing in the arms of the V-shape. The data for the Pedestal Paradigm showed a minimum at equal energy white, with shallower arms. We used a fixed adaptation chromaticity of equal energy white in conjunction with Eq. (7) to calculate OPP_C . The value of p in Eq. (7) was 0.45 for HS and 0.69 for HY.

DISCUSSION

The goal of our study was to understand the role of adaptation and surround structure on chromatic discrimination. We developed a model of retinal processing in order to evaluate the data. The model provides a unified approach to detection and discrimination. The model was optimized to predict data for a target replacing briefly a steadily viewed background (Pulse Paradigm). Based on literature data, we expected and found adaptation to the steady background. We found that the size and spatial structure of the background did not influence discrimination threshold. Thresholds were determined by the size of the spatio-temporal chromatic contrast step generated with respect to the background.

Our data indicate that even when the discrimination targets were presented steadily (Pedestal Paradigm) there was no evidence that cells adapted to the target chromaticity mediated the discriminations. Discrimination remained controlled by the surround even under the limiting condition that the display provided a narrow 0.07° crosshair separating the targets. We also confirmed previous experiments^{11,40} using steadily presented stimuli in an otherwise dark field. The V-shape suggested that in the dark, the parvocellular pathway shows an intrinsic normalization near equal energy white. The data contradict the intuitive view that adaptation to the test field chromaticity should determine discriminability. Rather, it is the adaptation to the surround that determines discriminability.

Chromatic discrimination improves with increase in target size (reviewed in Pokorny and Smith¹). The range of improvement has greater extent than is seen in threshold spatial summation studies.⁴¹ This result suggests that, for chromaticity discrimination, the visual system can use the information generated along the extensive borders of the discrimination targets.

Perhaps the most striking experimental results are that “the edge is all that matters” and that separations as small as 0.07° (4.2 min) can affect discriminative performance. Boy-

Surround: $2.07^\circ \times 2.07^\circ$

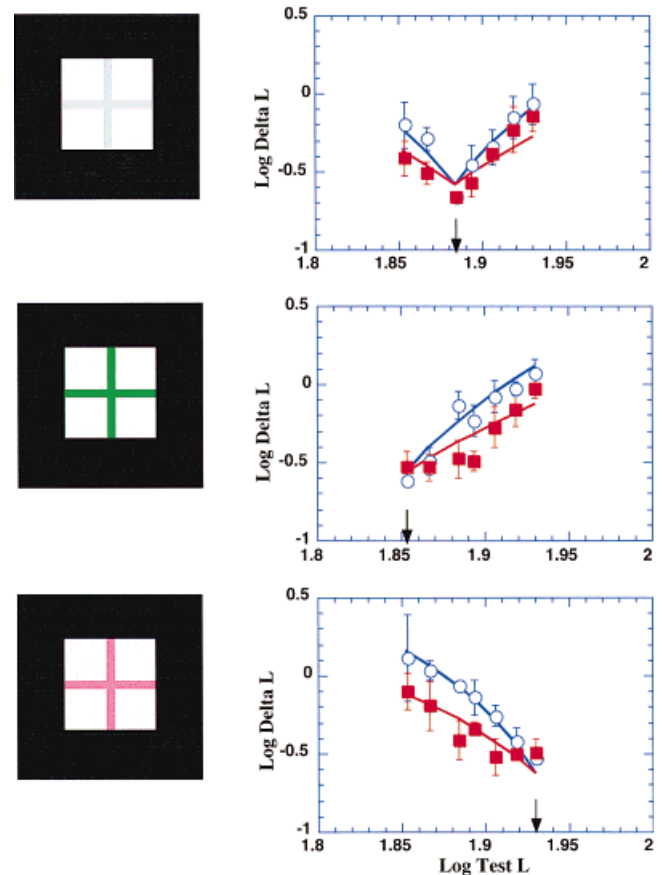


FIG 8. Discrimination data for a $2.07^\circ \times 2.07^\circ$ surround comparing both paradigms (observer HS). Format follows Fig. 6.

Surround: 2.07°x2.07° with black separations

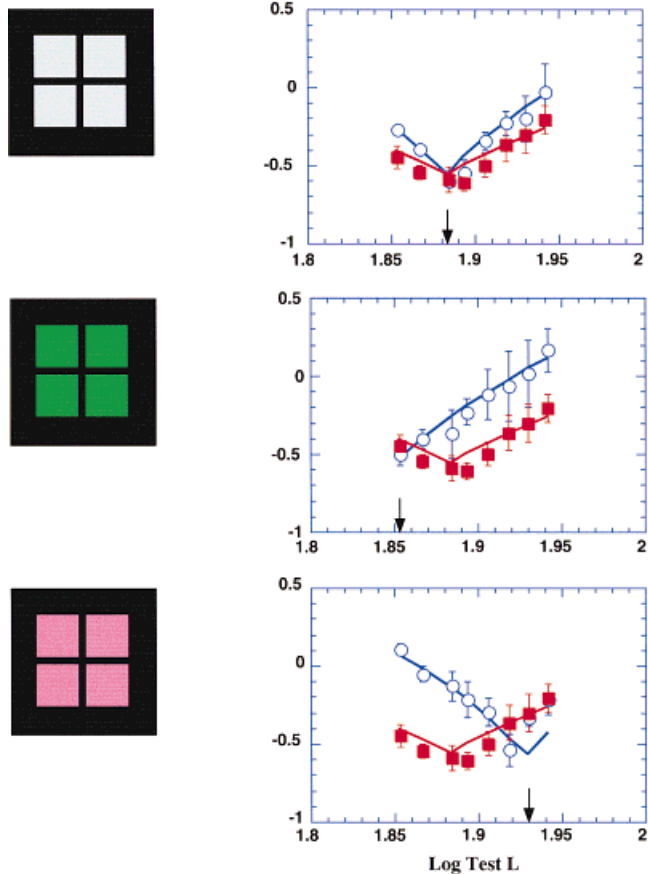


FIG 9. Discrimination data for a 2.07° surround and black separations, comparing both paradigms (observer HS). Format follows Fig. 6.

nton, Hayhoe, and MacLeod⁴⁶ investigated discrimination with and without the presence of gaps between adjacent fields. Using the method of adjustment and 1.2° fields, they observed that gaps as small as 2.7' led to degradations in equiluminant discriminations mediated by *L* and *M* cones. Our data provide an explanation of the “gap effect.” The gap provides a narrow neutral border. There is a contrast signal generated between the border and the chromatic test field. The contrast signal deteriorates discrimination for test chromaticities other than neutral. The importance of such very thin borders may seem contradicted by the poor chromatic visual acuity at equal luminance.⁴⁷ Our display was not periodic; the 4.2 min gap was visible for all displays with chromatic contrast between surround and test fields.

The PC-pathway model can be modified to predict increment detection on a steady background.⁴⁷ Under these conditions, we assume that a given PC-pathway cell is affected both by gain and by subtractive adaptation to the background. The increment threshold is now least sensitive at the adapting chromaticity, because a fixed retinal illuminance increment at the adapting chromaticity generates only a small signal in the PC-pathway. At other test chromaticities,

a fixed retinal illuminance increment generates a larger spectral opponent signal; thus, a lower test retinal illuminance should be required for detection. With an achromatic background, detection sensitivity above 500 nm showed a characteristic bi-lobed shape with minimum at the adapting chromaticity.^{50,51} The interpretation⁵¹ was that one or more PC-pathway opponent processes mediated detection in the lobes. Hue identification at threshold has confirmed this interpretation.⁵² It was assumed that a nonopponent process (the magno-cellular pathway) mediated detection at the adapting chromaticity.⁵¹ The relative sensitivities of the PC- and MC-pathways were determined by the spatio-temporal parameters of the test stimulus.⁵¹ Detection of a 200 msec square pulse gave an obvious bi-lobed function, while detection of a 10 msec square pulse was similar to that determined by flicker photometry. Miyahara⁴⁹ showed that, with a 1 Hz raised cosine, detection at the Sloan notch was mediated by the other spectral opponent channel, the koniocellular [$+S - (L+M)$] pathway. According to our model, PC-pathway detections mediated between 500 nm and the adapting chromaticity would be mediated by a [$+M - L$] and detections above the adapting chromaticity by a [$+L - M$] PC-pathway channel.

The PC-pathway cells may also be involved in Wald's test sensitivity approach using a fixed background wavelength with varying test wavelengths, and the Stiles field sensitivity approach using a fixed test wavelength with varying background wavelengths. As with detection on achromatic backgrounds, the relative sensitivities of the multiple pathways should depend on the spatio-temporal characteristics of the test stimulus. For the test sensitivity method, our PC-pathway model would predict bi-lobed functions with minimum at the adapting chromaticity. On a long wavelength adapting field, much of the curve would reflect activity in [$+M - L$] cell types, while on a short wavelength adapting field much of the curve would reflect activity in [$+L - M$] cell types. For the field sensitivity approach, the choice of test wavelength favors a role for [$+M - L$] for Π_4 and [$+L - M$] for Π_5 , respectively. For most literature data, an optimal PC-pathway stimulus was not used; the obtained functions probably represent some combination of PC- and MC-pathways.

ACKNOWLEDGMENTS

We thank Linda Glennie for technical assistance in programming the image processing systems and Steven K. Shevell for comments. We also thank our observers AC, YH, and GK for their patience and time.

1. Pokorny J, Smith VC. Colorimetry and color discrimination. Boff KR, Kaufman L, Thomas JP, editors. Handbook of perception and human performance, Vol. I: Sensory processes and perception. New York: Wiley; 1986. p 8-1–8-51.
2. Wright WD. The sensitivity of the eye to small colour differences. Proc Phys Soc 1941;53:93–112.
3. MacAdam DL. Visual sensitivities to color differences in daylight. J Opt Soc Am 1942;32:247–274.

4. Proc. of the 8th session, CIE, Cambridge, September 1931. Cambridge: Cambridge University Press; 1932. p 19.
5. Helmholtz H. *Handbuch der Physiologischen Optik*. 2nd Ed. 1896.
6. Schrödinger E. *Grundlinien einer Theorie der Farbenmetrik im Tagessehen*. *Ann Physik* 1920;63:481. (English translation in MacAdam DL, editor. *Sources of color science*. Cambridge, MA: MIT Press. *Ann Physik*. Vol. 63; 1920. p 134–182.
7. Stiles WS. A modified Helmholtz line-element in brightness-colour space. *Proc Phys Soc* 1946;58:41–65.
8. Stiles WS. The line element in colour theory: A historical review. Vos JJ, Friele LF, Walraven CPL, editors. *Color metrics*. Soesterberg: AIC/Holland; 1972. p 1–25.
9. Jameson D, Hurvich LM. Some quantitative aspects of an opponent-colors theory I. Chromatic responses and spectral saturation. *J Opt Soc Am* 1955;45:546–552.
10. LeGrand Y. Les seuils différentiels de couleurs dans le théorie de Young. (English translation by K. Knoblauch. *Color difference thresholds in Young's theory*. *Col Res Appl* 1994;19:296–309). *Revue d'Optique* 1949;28:261–278.
11. Boynton RM, Kambe N. Chromatic difference steps of moderate size measured along theoretically critical axes. *Col Res Appl* 1980;5:13–23.
12. Smith VC, Pokorny J. Spectral sensitivity of the foveal cone photopigments between 400 and 500 nm. *Vision Res* 1975;15:161–171.
13. MacLeod DIA, Boynton RM. Chromaticity diagram showing cone excitation by stimuli of equal luminance. *J Opt Soc Am* 1979;69:1183–1185.
14. Smith VC, Pokorny J. The design and use of a cone chromaticity space. *Col Res Appl* 1996;21:375–383.
15. Lee BB. Receptive field structure in the primate retina. *Vision Res* 1996;36:631–644.
16. Dacey DM. Circuitry for color coding in the primate retina. *Proc Natl Acad Sci* 1996;93:582–588.
17. Derrington AM, Krauskopf J, Lennie P. Chromatic mechanisms in lateral geniculate nucleus of macaque. *J Physiol* 1984;357:241–265.
18. Lee BB, Pokorny J, Smith VC, Kremers J. Responses to pulses and sinusoids in macaque ganglion cells. *Vision Res* 1994;34:3081–3096.
19. Kuffler SW. Neurons in the retina: organization, inhibition and excitation problems. *Cold Spring Harbor Symp Quant Bio* 1952;17:281–292.
20. Derrington AM, Lennie P. The influence of temporal frequency and adaptation level on receptive field organization of retinal ganglion cells in cat. *J Physiol* 1982;333:343–366.
21. Martin PR, White AJ, Goodchild AK, Wilder HD, Sefton AE. Evidence that blue-on cells are part of the third geniculocortical pathway in primates. *Euro J Neurosci* 1997;9:1536–1541.
22. Smith VC, Glennie L, Pokorny J. Color discrimination and color appearance in the equiluminant plane. *Invest Ophthalmol Vis Sci Suppl* 1994;35:2167.
23. Smith VC, Pokorny J. Data and prediction of color discrimination. *OSA Annual Meeting/ILS-XIV Program* 1998;54.
24. Sun H, Smith VC, Pokorny J. Decreasing surround size fails to alter chromatic discrimination. *Invest Ophthalmol Vis Sci Suppl* 1998;39: S162.
25. Vos JJ. Colorimetric and photometric properties of a 2° fundamental observer. *Col Res Appl* 1978;3:125–128.
26. LeGrand Y. *Light, colour and vision*. Second Ed. London: Chapman Hall; 1968. p 1–564.
27. Gille JL. Evaluation of a general model of color vision using detection and identification on narrowband increments to a neutral background. *Univ California, Los Angeles*, 1984.
28. Lee BB, Pokorny J, Smith VC, Martin PR, Valberg A. Luminance and chromatic modulation sensitivity of macaque ganglion cells and human observers. *J Opt Soc Am A* 1990;7:2223–2236.
29. Zaidi Q, Shapiro A, Hood D. The effect of adaptation on the differential sensitivity of the S-cone color system. *Vision Res* 1992;32: 1297–1318.
30. Stiles WS. Color vision: The approach through increment threshold sensitivity. *Proc Natl Acad Sci* 1959;45:100–114.
31. Wald G. The receptors of human color vision. *Science* 1964;145:1007.
32. Swanson WH, Ueno T, Smith VC, Pokorny J. Temporal modulation sensitivity and pulse detection thresholds for chromatic and luminance perturbations. *J Opt Soc Am A* 1987;4:1992–2005.
33. Yeh T, Lee BB, Kremers J. Time course of adaptation following luminance and chromatic change. *Vision Res* 1996;36:913–931.
34. Shapley R. Visual sensitivity and parallel retinocortical channels. *Ann Rev Psych* 1990;41:635–658.
35. Hood DC. Psychophysical and electrophysiological tests of physiological proposals of light adaptation. *Visual psychophysics: its physiological basis*. Armington J, Krauskopf J, Wooten B, editors. New York: Academic; 1978. p 141–155.
36. Hood DC, Ilves T, Maurer E, Wandell B, Buckingham E. Human cone saturation as a function of ambient intensity: a test of models of shifts in the dynamic range. *Vision Res* 1978;18:983–993.
37. Hood DC, Finkelstein MA, Buckingham E. Psychophysical tests of models of the response-intensity function. *Vision Res* 1979;19:401–406.
38. Hayhoe M, Benimoff NI, Hood DC. The time-course of multiplicative and subtractive adaptation processes. *Vision Res* 1987;27:1981–1996.
39. Yeh T. *Colorimetric purity discrimination: theory and data*. Dissertation. Univ Chicago; 1991.
40. Miyahara E, Smith VC, Pokorny J. How surrounds affect chromaticity discrimination. *J Opt Soc Am A* 1993;10:545–553.
41. Hood DC, Finkelstein MA. Sensitivity to light. Boff KR, Kaufman L, Thomas JP, editors. *Handbook of perception and human performance*. Vol I: Sensory processes and perception. New York: Wiley; 1986. p 5-1–5-66.
42. Smith VC, Lee BB, Pokorny J, Martin PR, Valberg A. Responses of macaque ganglion cells to the relative phase of heterochromatically modulated lights. *J Physiol* 1992;458:191–221.
43. Watanabe A, Pokorny J, Smith VC. Red-green chromatic discrimination with variegated and homogeneous stimuli. *Vision Res* 1998;38: 3271–3274.
44. Kremers J, Lee BB, Pokorny J, Smith VC. Responses of macaque ganglion cells and human observers to compound periodic waveforms. *Vision Res* 1993;33:1997–2011.
45. Krauskopf J, Gegenfurtner K. Color discrimination and adaptation. *Vision Res* 1992;32:2165–2175.
46. Boynton RM, Hayhoe MM, MacLeod DIA. The gap effect: chromatic and achromatic visual discrimination as affected by field separation. *Optica Acta* 1977;24:159–177.
47. Mullen KT. The contrast sensitivity of human colour vision to red-green and blue-yellow chromatic gratings. *J Physiol* 1985;359:381–400.
48. Yeh T, Smith VC, Pokorny J. Colorimetric purity discrimination: data and theory. *Vision Res* 1993;33:1847–1857.
49. Miyahara E, Pokorny J, Smith VC. Increment threshold and purity discrimination spectral sensitivities of X-chromosome-linked color defective observers. *Vision Res* 1996;36:1597–1613.
50. Sperling HG, Harwerth RS. Red-green cone interaction in the increment-threshold spectral sensitivity of primates. *Science* 1971;172: 180–184.
51. King-Smith PE, Carden D. Luminance and opponent-color contributions to visual detection and adaptation and to temporal and spatial integration. *J Opt Soc Am* 1976;66:709.
52. Thornton JE, Pugh EN Jr. Relationship of opponent colours cancellation measures to cone-antagonistic signals deduced from increment threshold data. Mollon JD, Sharpe LT, editors. *Colour vision: physiology and psychophysics*. London: Academic; 1983. p 361–383.